International Journal of Computer Assisted Radiology and Surgery (2018) 13:769–776
https://doi.org/10.1007/s11548-018-1745-3

ORIGINAL ARTICLE

Blended shared control utilizing online identification

Regulating grasping forces of a surrogate surgical grasper

Trevor K. Stephens[1] · Nathan J. Kong[1] · Rodney L. Dockter[1] · John J. O'Neill[1] · Robert M. Sweet[2] · Timothy M. Kowalewski[1]

Received: 29 January 2018 / Accepted: 20 March 2018 / Published online: 28 March 2018

Abstract

Purpose Surgical robots are increasingly common, yet routine tasks such as tissue grasping remain potentially harmful with high occurrences of tissue crush injury due to the lack of force feedback from the grasper. This work aims to investigate whether a blended shared control framework which utilizes real-time identification of the object being grasped as part of the feedback may help address the prevalence of tissue crush injury in robotic surgeries.

Methods This work tests the proposed shared control framework and tissue identification algorithm on a custom surrogate surgical robotic grasping setup. This scheme utilizes identification of the object being grasped as part of the feedback to regulate to a desired force. The blended shared control is arbitrated between human and an implicit force controller based on a computed confidence in the identification of the grasped object. The online identification is performed using least squares based on a nonlinear tissue model. Testing was performed on five silicone tissue surrogates. Twenty grasps were conducted, with half of the grasps performed under manual control and half of the grasps performed with the proposed blended shared control, to test the efficacy of the control scheme.

Results The identification method resulted in an average of 95% accuracy across all time samples of all tissue grasps using a full leave-grasp-out cross-validation. There was an average convergence time of 8.1 ± 6.3 ms across all training grasps for all tissue surrogates. Additionally, there was a reduction in peak forces induced during grasping for all tissue surrogates when applying blended shared control online.

Conclusion The blended shared control using online identification more successfully regulated grasping forces to the desired target force when compared with manual control. The preliminary work on this surrogate setup for surgical grasping merits further investigation on real surgical tools and with real human tissues.

Keywords Shared control · Robotic surgery · Tissue identification · Tissue crush injury

Introduction

Although surgeons utilize surgical robots for improved dexterity, scalable movements, and enhanced vision, the current surgeon-robot setup is not immune to errors. An increase of adverse event risk was reported the same year that robotic-assisted minimally invasive surgeries (RMIS) were infused nationally for the use in radical prostatectomy [9]. Additionally, a comparison of robotic sutures to hand sutures showed that the exerted forces were much greater during RMIS [10].

Current robotic surgeries operate under a master-slave setup. The master (surgeon) sends commands to the slave (robot) which are followed indiscriminately. In this setup, the robot acts merely as a passive tool, despite the fact that

Research was sponsored in part by the National Science Foundation Graduate Research Fellowship under Grant No. 00039202. Any opinion, findings, and conclusions or recommendations expressed in this material are those of the authors and do not necessarily reflect the views of the National Science Foundation.

✉ Trevor K. Stephens
steph594@umn.edu

[1] Department of Mechanical Engineering, University of Minnesota, Minneapolis, MN, USA

[2] Department of Urology, University of Washington, Seattle, WA, USA

these surgical robots possess sensors, and with appropriate algorithms could exhibit intelligence. Sie et al. [13] propose tissue-aware surgical robots as a possible enhancement to current surgical robots. Their preliminary work showed that tissue identification is possible during surgical grasping [13]. They propose the idea to utilize this identification in a control loop to regulate grasping forces to tissue-specific levels. A benefit of this could be to reduce tissue crush injury, which is caused by excess forces during grasping [1]. De et al. [1] presented work on finding tissue-specific thresholds for tissue crush injury, which would provide target grasping forces in conjunction with real-time identification.

In the current state, the ability to prevent excessive force during RMIS, and thus prevent tissue crush injury, is merely a proposed idea. This work aims to further explore the feasibility of this idea by incorporating real-time identification as feedback in a human-in-the-loop (HitL) blended shared control architecture to limit grasping forces. This work focuses on an RMIS surrogate setup, with a custom teleoperated grasper as a surrogate for a surgical robot, and two silicone-based synthetic tissues as surrogates for human tissues. The main contributions of this work include (1) a shared control scheme that blends HitL position control with computationally derived implicit force control; (2) convexly weighted arbitration derived from confidence in a proposed tissue identification algorithm; and (3) an online tissue identification algorithm based on a nonlinear tissue model. We hypothesize that incorporating tissue identification as feedback in HitL blended shared control more effectively regulates grasping forces to a pre-defined force level than human-only control in our surrogate setup.

Background

A key weakness in both robotic and laparoscopic surgery is the lack of haptic feedback. This can prevent surgeons from using their sense of touch in order to assess potential complications [15]. Additionally, the lack of sensing can lead surgeons to grasp tissue too hard, thus causing tissue crush injuries [1,16]. In laparoscopic cholecystectomies, laparoscopic graspers have been shown to increase tissue crush injuries significantly [8,11]. Similarly, laparoscopic gynecological procedures result in a 1.5% rate of injury to the ureter, resulting in inflammation, cellular death, and fistula formation [12]. For colorectal surgeries, one of the most common instrument-induced injuries is inadvertent tearing of the bowel from grasping too hard [14]. The tissue crush injuries revealed in these studies are often largely attributed to the minimal force feedback available to surgeons with laparoscopic tools, which is a problem even further exacerbated in RMIS.

Several studies have focused on the quantitative benefits that force feedback can provide. MacFarlane et al. designed a custom Babcock grasper with force feedback and a haptic control console in order to test how well subjects could identify the compliance (i.e., firmness) of sample tissue [7]. When compared with a standard grasper, the force feedback grasper reduced the mean square error in compliance identification approximately fourfold. Tholey et al. performed a similar study to evaluate the effects of vision, force, and combined feedback in regard to identification of tissue stiffness [15]. Their study indicated that vision feedback resulted in a 52% tissue classification rate while force feedback and combined feedback resulted in a 67 and 83% classification rate, respectively.

Wagner et al. evaluated the amount of force applied to tissue using a surgical robotic system during a mock blunt dissection and compared the results using various amounts of force feedback [16]. The results showed that without force feedback, subjects applied an average force magnitude which was 50% greater than with force feedback. The peak force magnitude similarly increased by 100% without force feedback. Additionally, the number of errors that resulted in damaged tissue increased threefold.

These instrumented approaches have yielded varying levels of success, but still rely on surgeons to respond to haptic cues. This may be difficult in an operating room which is already inundated by various sensory signals being sent to a surgeon. An alternative approach is to incorporate intelligence garnered by sensors on the robot as feedback in a blended shared control scheme, which would regulate grasping forces in conjunction with human efforts. This HitL framework aims at combining the strengths of a human (acuity and decision making) with advantages from computational intelligence (precision and repeatability).

Shared control has been studied extensively in various robotic applications outside of surgery. Enes and Book highlight six arbitration schemes with detailed example of each in [4]. Of these six, we apply blended shared control to the grasping problem. In blended shared control, an arbitration function is used to convexly weight control authority between human and computational intelligence.

Dragan and Srinivasa assess the concept of assistance in shared control, and how this most effectively relates to arbitration [3]. They do this both in relation to the confidence in robot-prediction as well as in user-preference of arbitration aggressiveness between varying levels of task difficulty. The main assertion from their work which we rely on is that arbitration should increase monotonically with confidence. This is a guiding principle for designing the arbitration function used in this work.

Our objective is to determine whether HitL blended shared control mitigates excessive tissue-specific grasping forces in simulated surgical robotic grasping to establish preliminary

evidence that this is a viable solution to apply to RMIS to help mitigate excessive grasping forces in the absence of haptic feedback.

Methods

Hardware

We developed a custom setup which acted as a surrogate for surgical grasping. The setup utilized a master-slave configuration to replicate teleoperation. A two-finger grasp controller functioned as the master. This consisted of two links that rotate about a rotary encoder (AMT 102, CUI Inc.) as shown in Fig. 1b. The sensed angle of the encoder served as the commanded angle for the slave grasper for direct position control of the grasper. The slave component (Fig. 1a) consisted of two DC motors (DCX 19 S, Maxon Precision Motors Inc.) which actuated each side of the grasper independently as well two encoders (AMT 102, CUI Inc.) to measure position on the grasping side. Each motor shaft was attached to a beam load cell (Phidgets 3130 Phidgets Inc.), with the load cell acting as the grasper arm to measure the force of each grasp directly. This setup allowed for direct measurements at the surrogate tissue-tool interface, which is not completely analogous to a surgical setup, as current surgical robots lack distal-end sensors at the grasping site. However, recent work has shown methods for accurately estimating end-effector force via back-end measurements alone on real surgical tools [6]. Additionally, in our previous work it was shown that identification of cadaveric tissue was successfully discriminated through back-end sensors alone using a da Vinci surgical tool [2].

Identification algorithm

The identification of surrogate tissues was performed using the force and position data collected by the slave grasper in conjunction with a nonlinear tissue model. The model is derived in Eqs. (1–7). The model stems from a tissue model from Fung [5]. When dynamic terms are relevant, we propose augmenting this model with dynamic terms as originally suggested by Yu et al. [18]. However, with these silicone tissue phantoms the nonlinear elastic response dominated and we were able to neglect these dynamic terms shown in Eq. (1). Our previous work has shown that these terms are not negligible in cadaveric tissues [2] and should therefore be included when appropriate:

$$\sigma = \overbrace{\frac{M\ddot{p}}{A} + \frac{D\dot{p}}{A}}^{\text{Linear dynamic terms [18]}} + \overbrace{\alpha(e^{\beta\epsilon} - 1)}^{\text{Nonlinear soft tissue terms [5]}} \quad (1)$$

where σ, is tissue compressive stress; M, is mass of the tissue; D, is damping of the tissue; p, is position of the grasper; A, is grasper area in contact with the tissue; α, β, are parameters of tissue stiffness; ϵ, is tissue strain.

We first neglect the dynamic terms as explained previously. Then, to perform tissue identification in the least squares sense, the nonlinear term was made linear in parameters via a third-order Taylor series expansion:

$$\sigma \approx k_3\epsilon^3 + k_2\epsilon^2 + k_1\epsilon + k_0 \quad (2)$$

Note this Taylor series expansion was centered around an arbitrary strain value. By expanding about a value of $\epsilon = 0$, the k_0 term would evaluate to zero. For this experimentation, the grasping area was kept constant and all surrogate

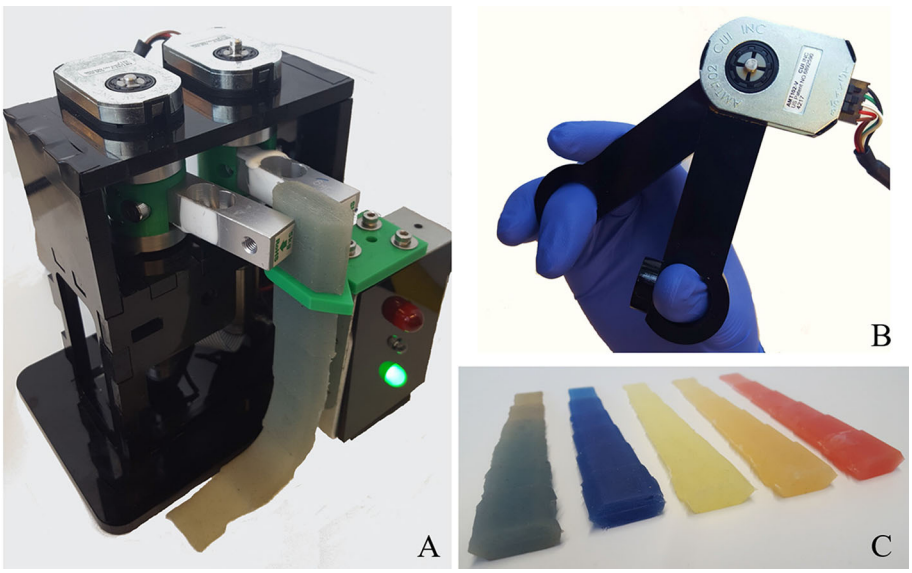

Fig. 1 Experimental setup with **a** slave-side hardware, **b** master-side hardware and **c** five synthetic tissue phantoms

tissues were of the same thicknesses. Therefore, the analogous force–displacement model can be used as shown in Eq. 3:

$$F \approx k_3 x^3 + k_2 x^2 + k_1 x + k_0 \tag{3}$$

Here, x represents the sensed angle, in radians, and F represents the force in Newtons as measured by the load cell. The values at first touch for x and F are 0 radians and 0 Newtons, respectively. The angle decreased as the grasp closed, whereas the force increased. To determine the class descriptor parameters, a training data set was populated using grasping data from all five surrogate tissues. This training data set was used to learn the representative class parameters $\Phi_{(i)}$, for each of the i classes:

$$\Phi_{(i)} = [\, k_{3(i)}\ k_{2(i)}\ k_{1(i)}\ k_{0(i)}]^T \tag{4}$$

To determine the parameters that minimize error from the training data, we utilized a least squares approach in which we populated a data matrix, $X(t)$, for a given surrogate tissue across each time step:

$$X(t) = \begin{bmatrix} x^3(t_0) & x^2(t_0) & x(t_0) & 1 \\ x^3(t_1) & x^2(t_1) & x(t_1) & 1 \\ \vdots & \vdots & \vdots & \vdots \\ x^3(t_n) & x^2(t_n) & x(t_n) & 1 \end{bmatrix} \tag{5}$$

We also populated a data vector, $F(t)$, for the same surrogate tissue at each time step:

$$F(t) = [F(t_0)F(t_1)\ldots F(t_n)]^T \tag{6}$$

The parameters were solved per the standard least squares solution, where the t has been dropped for brevity:

$$\Phi_{(i)} = \left(X_{(i)}^T X_{(i)}\right)^{-1} X_{(i)}^T F_{(i)} \tag{7}$$

This process was repeated for all classes to obtain representative class parameters for each of the five surrogate tissues. Once the training parameters were computed for each class, they were used online for identification. Identification was performed by identifying the class with minimum error as computed by:

$$e_{(i)} = \sum_{t=t_0}^{t_n} \left| F(t) - X(t)\Phi_{(i)} \right| \tag{8}$$

Here, $e_{(i)}$ is the cumulative classification error for the ith class given previously unseen data $X(t)$ and $F(t)$. Using this value, the class with the lowest cumulative error was assumed to be the tissue class. For example, if e_3 had the lowest cumulative error of the five classes, then the estimated tissue type is class 3. Along with the estimated tissue type, a confidence value for each class, $\alpha_i \in [0, 1]$, was also computed. This confidence was calculated as follows:

$$\alpha_i = \frac{\frac{1}{e_i}}{\sum_{k=1}^{5} \frac{1}{e_k}} \tag{9}$$

The value of α corresponding to the estimated class also represents the arbitration variable, which monotonically increases with confidence of the prediction as established in [3]. These error values were also used to empirically determine the convergence rate of classification. Convergence was defined as the final time step at which the prediction did not classify correctly (i.e., after this point, the prediction was never incorrect again).

In addition to the tissue type and the confidence value, this algorithm also returns a tissue-specific force target which corresponds to the estimated tissue type. This value (F_{target}) was passed to the shared control algorithm to limit grasping force.

Five synthetic tissue samples were utilized (Fig. 1c) to implement and test the tissue identification algorithm. These tissue surrogates were created using combinations of silicone rubber and deadener (PlatSil®) in combinations as shown in Table 1. The tissue samples ranged in stiffness from lowest to highest (green, blue, yellow, orange, red), with a continuum of properties in between. A total of 30 training grasps were collected for each tissue type to learn classification parameters.

Using the training grasp data for each tissue, the least squares training algorithm was used to compute representative class parameters for each tissue type (Eq. 7). The parameters were computed 30 times where each computation left one of the grasps out. The average class parameter values along with associated standard deviations are reported in Table 2.

The blended shared control scheme is shown in Fig. 2. The input to the system is a convex weighting of human-

Table 1 Computed parameters for five synthetic tissue with standard deviations

Green	Blue	Yellow	Orange	Red
PlatsilGel OO + 100% deadener	PlatsilGel OO + 50% deadener	PlatsilGel OO	PlatsilGel 10 + 25% deadener	PlatsilGel 10

Table 2 Computed parameters for five synthetic tissues with standard deviations

	k_3 (N)	k_2 (N)	k_1 (N)	k_0 (N)
Φ_{green}	− 20,030 ± 150	− 2217 ± 25	− 101.8 ± 0.9	− 0.8787 ± 0.0082
Φ_{blue}	− 18,330 ± 190	− 1317 ± 23	− 92.69 ± 0.70	− 0.3404 ± 0.0060
Φ_{yellow}	− 14,480 ± 200	− 598.8 ± 18.7	− 85.91 ± 0.52	− 0.3106 ± 0.0045
Φ_{orange}	− 7521 ± 265	272.9 ± 28.2	− 72.24 ± 0.85	0.0864 ± 0.0064
Φ_{red}	− 10,740 ± 250	297.5 ± 24.3	− 103.7 ± 0.6	− 0.2002 ± 0.0045

Fig. 2 Shared control scheme

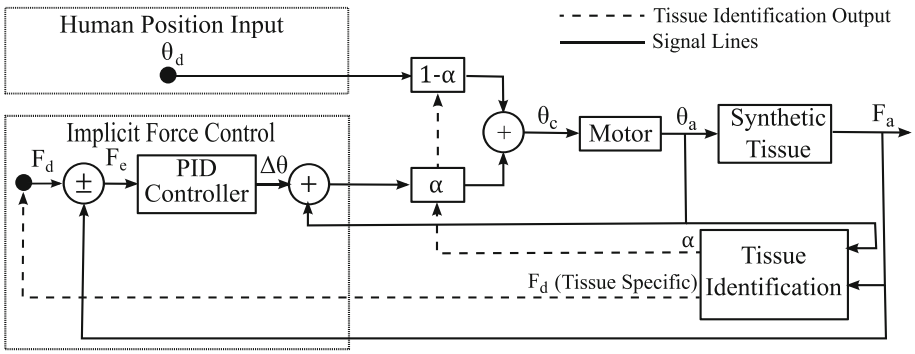

Table 3 Classification results for five synthetic tissues

$N = 17{,}868$	Actual[a]					Total	Precision
	Green	Blue	Yellow	Orange	Red		
Predicted							
Green	3579	0	0	0	0	3579	1.0
Blue	66	3366	169	6	31	3638	0.93
Yellow	0	232	3228	34	40	3534	0.91
Orange	0	0	0	3372	18	3390	0.99
Red	0	19	20	269	3419	3727	0.92
Total	3645	3617	3417	3681	3508		
Recall	0.98	0.93	0.94	0.92	0.97		

[a]Analysis was done on a per time-step basis across all time steps of every grasp (N = 17,868); classification results on a per grasp basis resulted in 100% accuracy for all five synthetic tissues

commanded position from the slave and calculated position from an implicit force controller [17]. The convex weighting is based on α, which is a confidence value returned from the tissue identification algorithm (Eq. 9). When $\alpha = 0$, control is taken directly from the human (fully manual). Conversely, when $\alpha = 1$, control is taken fully from the robot (fully autonomous). The complete controller equation is given in Eq. (10):

$$\theta_c(t) = (1-\alpha(t))\theta_d(t) + \alpha\left(K_p(F_e(t)) + K_i\int_0^t F_e(t)(\tau)\mathrm{d}\tau + K_d\frac{\mathrm{d}F_e(t)}{\mathrm{d}t} + \theta_a(t)\right) \quad (10)$$

The tissue identification algorithm also returns a tissue-specific force target (F_{target}). The difference between this target and the measured force is the error signal for the controller. The controller is a proportional-integral (PID) controller, which was tuned using the heuristic Ziegler–Nichols approach with α set to one.

Each grasp of the training data was evaluated for tissue classification estimates at each time step in order to examine the recall and precision. A confusion matrix for the full leave-grasp-out cross-validation is presented in Table 3.

Separate grasps, which were not included in training, were used to test the efficacy of the shared control. A total of twenty grasps were performed, half with and half without shared control, for all five tissue types. For these online tests, we assumed to know the model parameters for the green, yellow, and red tissues, but purposely did not include model parameters for the blue and orange classes. This allowed us to test three known classes and two unknown classes, to mimic what may happen when an unknown tissue is encountered in a surgical setting. The pre-determined thresholds for the green, yellow, and red tissue surrogates were arbitrarily chosen at 6.9, 8.3, and 9.8 N, respectively. Since we treated the blue

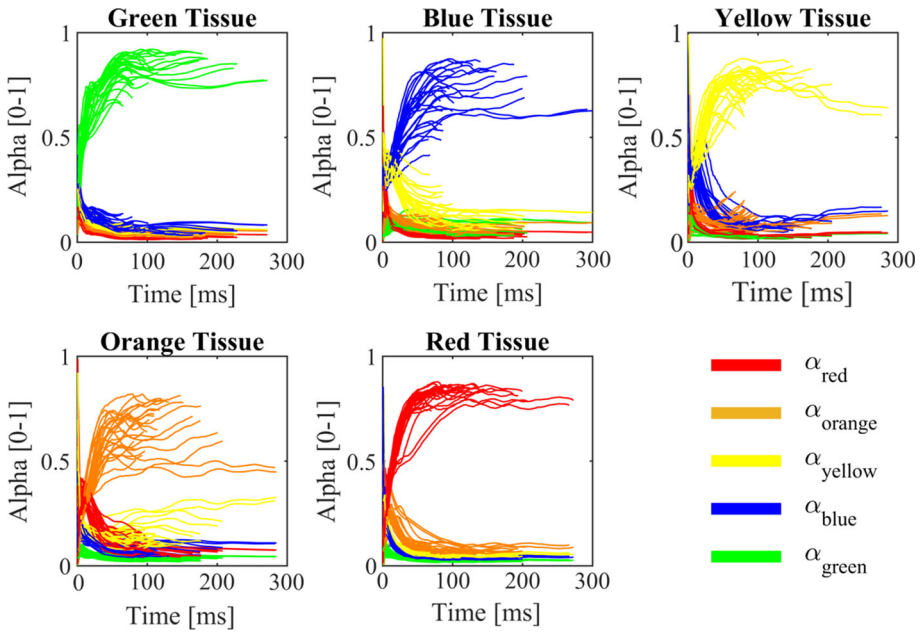

Fig. 3 Computed alpha confidence for all 30 grasps on each colored tissue surrogate

Table 4 Computed convergence times for five synthetic tissues with standard deviations

Green (ms)	Blue (ms)	Yellow (ms)	Orange (ms)	Red (ms)
2.4 ± 1.5	12 ± 8	9.7 ± 5.7	12 ± 4	4.1 ± 2.4

and orange tissue surrogates as unknown, these tissues did not have associated force targets, but instead were assigned a target from whichever of the three known classes it was identified as at each time step.

Results

The table of classification results for each tissue type is included in Table 3 as a confusion matrix. For each training grasp, the confidence values (α) were also recorded. Each of these alpha values for all five tissue surrogates across all grasps is included in Fig. 3. The mean convergence times with associated standard deviations are also reported in Table 4.

The results from the online grasping with and without shared control are shown in Fig. 4. The left column of plots represents the three classes which were treated as previously known and trained, whereas the right column of plots represents the two classes which were treated as unknown and untrained.

Discussion

The results from the tissue identification approach indicate an improvement in accuracy and convergence time for classification. Classification accuracy for all five tissue surrogates is on average 95% accurate. This analysis includes all time steps and therefore is bolstered by the consistently accurate estimates which occur in the latter portion of the grasp, after more information has been obtained. However, we also report an average classification convergence time of 8 ms across all tissue types, with the worst average convergence time being the blue tissue at 12 ms. This shows that accurate classification is occurring during the early portion of grasps. This is a marked improvement over previously reported work. Sie et al. achieved classification convergence within 300 ms using the Smart Tool platform [13]. This may be because our hardware provides inherently lower noise due to the decoupling of the force measurement from the kinematic chain. Also, the synthetics used in this experiment are likely easier to classify than the porcine tissue used previously. Our least squares classification scheme can be readily adapted to the surgical grasper platform and used for tissue identification in that setting. The plots of the alpha confidence value (Fig. 3) indicate a smooth increase in confidence as the classification convergences, which aligns with the notion of arbitration monotonically increasing with confidence as asserted by Dragan and Srinivasa [3]. Additionally, this increase in confidence is ideal for this application of shared control since more weighting will be given to the computational force controller as the grasp trajectory settles.

This shared control scheme is, to our knowledge, the first shared control scheme used to target grasping forces by blending human position control with computational implicit force control. With this shared control scheme, there is a

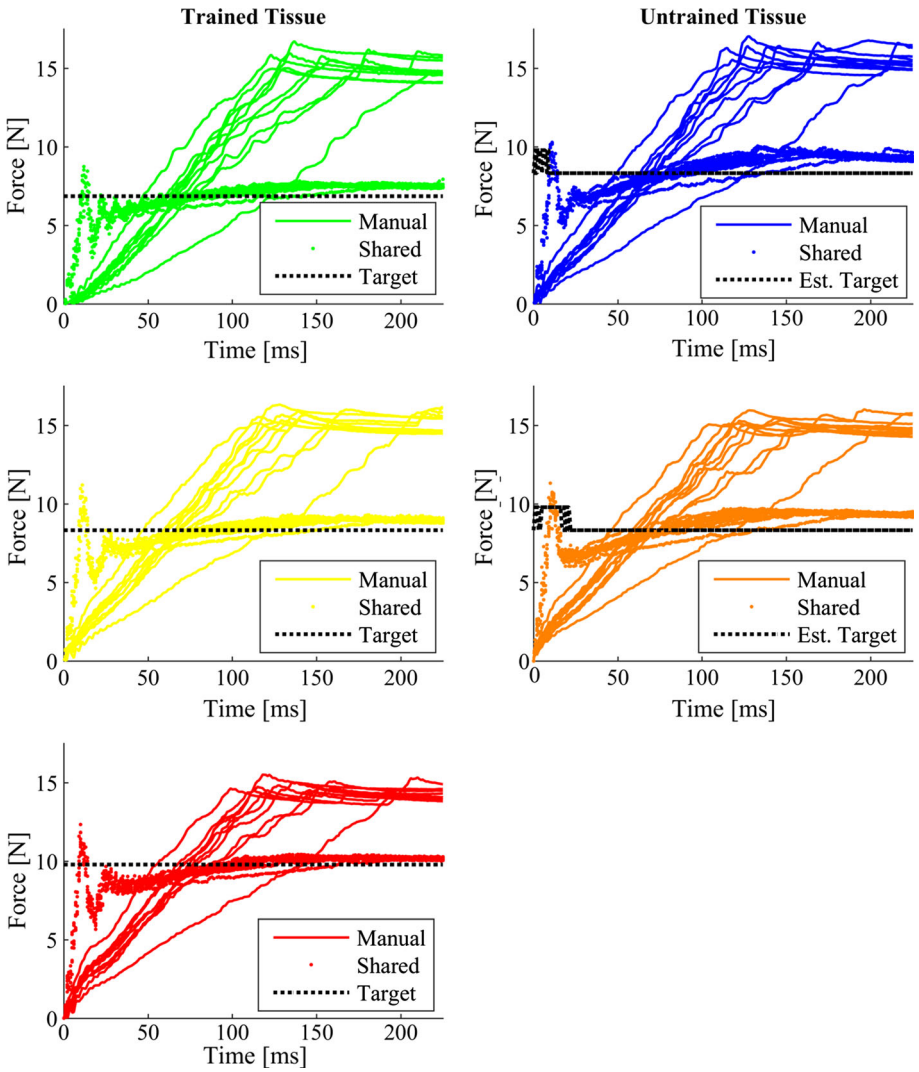

Fig. 4 Grasping data with and without shared control for all twenty grasps. The left column represents the three classes which were trained (green, yellow, and red). These all have fixed targets based on their tissue type. The right column represents the two classes which were untrained (blue and orange). These both have estimated targets which can change at each time step based on the current estimation

marked reduction in peak forces over human-only grasps. This reduction in peak force can be adjusted based on the pre-determined force targets. The benefit of this is seen when trying to prevent tissue crush injury. For more delicate tissues, the force target could be set lower to avoid tissue crush injury. The shared control scheme as manifested in these experiments shows potential for effectively regulating force, therefore limiting tissue crush injury.

For these initial results, arbitrary values were used for the force targets. However, this platform could easily be extended to utilize tissue-specific force targets as determined by thresholds from De et al. [1]. In this manner, the force targets would correspond directly to the tissue type that has been identified to appropriately mitigate tissue crush injury.

There are several limitations to this work. First, the tissues used in this experimentation are synthetic silicones. While these were created to roughly match differences between real tissues, they may inadequately represent true tissues—particularly in vivo tissues found in surgery. We anticipate that translating this work directly to in vivo tissues would drastically decrease identification confidence, as the inhomogeneity and large variance in tissue properties would result in blurred boundaries between tissue types. Despite this less accurate identification confidence, this methodology could still improve upon the current situation where there is no intervening machine autonomy. For instances where the identification accuracy is high, the target force can be reached as shown with this work. In cases where there is low identification accuracy, the algorithm reverts back to the surgeon and the performance is just as good as the current state of the art for grasping. We do not anticipate this methodology to help grasping every single time, but if, for example, it is able to mitigate to the proper grasping force one out of ten times, it still is an improvement over the current grasping done in surgery.

Additionally, our treatment of unknown or unexpected tissues requires further development. Notably, if an unknown class is identified, instead of forcing classification to its most

similar counterpart and using that target force, reverting full control back to the clinician may be more suitable in surgical settings.

The next limitation is that the hardware is not a surgical tool and may not accurately represent sensing actually available at the site of grasping in surgical procedures. The conclusions of this work therefore cannot translate directly to surgical contexts, though they motivate further exploration. Overall, the improvements in peak force reduction and tissue classification times were significant over prior art.

Conclusions

This work presents multiclass classification and a shared control scheme to regulate force to an optimal target dependent on the identification of the grasped object. This work shows promise for the surrogate surgical setup, which motivates exploration of this work on surgical equipment. It supports the hypothesis that incorporating tissue identification as feedback in HitL blended shared control more effectively regulates grasping forces to a pre-defined force level than human-only control for the surrogate surgical setup. Once this work transitions to a surgical tool, tissue identification and force targets can be related to specific anatomy, which would provide more clinical relevance.

The surgical application of this work focuses on prevention of tissue crush injury within this surrogate setup. Although tissue crush injury is prevalent within robotic surgeries, it is typically not a fatal surgical error. However, this work can be further investigated with more life-threatening errors such as puncturing blood vessels. The same concepts can be extended to these cases, but new techniques need to be established in sensing these errors for a shared control scheme to work. This work introduces a framework to continue and expand such efforts.

Funding This material is based upon work supported by the National Science Foundation Graduate Research Fellowship under Grant No. 00039202. Any opinion, findings, and conclusions or recommendations expressed in this material are those of the authors and do not necessarily reflect the views of the National Science Foundation.

Compliance with ethical standards

Conflict of interest Robert Sweet is a consultant for Olympus-Advisory for endourologic applications. Robert Sweet is chief executive officer for Simagine Health-Distributing simulation training solutions.

Ethical standard This article does not contain any studies with human participants or animals performed by any of the authors.

Informed consent This articles does not contain patient data.

References

1. De S, Rosen J, Dagan A, Hannaford B, Swanson P, Sinanan M (2007) Assessment of tissue damage due to mechanical stresses. Int J Robot Res 26(11–12):1159–1171
2. Dockter R, O'Neill J, Stephens T, Kowalewski T (2016) Feasibility of tissue classification via da vinci endowrist surgical tool. In: Hamlyn symposium on medical robotics, pp 64–65
3. Dragan AD, Srinivasa SS (2013) A policy-blending formalism for shared control. Int J Robot Res 32(7):790–805
4. Enes A, Book W (2010) Blended shared control of zermelo's navigation problem. In: American control conference (ACC), 2010, IEEE, pp 4307–4312
5. Fung Y (1981) Biomechanics: mechanical properties of living tissues. Springer, New York
6. Li Y, Hannaford B (2017) Gaussian process regression for sensorless grip force estimation of cable-driven elongated surgical instruments. IEEE Robot Autom Lett 2(3):1312–1319
7. MacFarlane M, Rosen J, Hannaford B, Pellegrini C, Sinanan M (1999) Force-feedback grasper helps restore sense of touch in minimally invasive surgery. J Gastrointest Surg 3(3):278–285
8. Marucci DD, Shakeshaft AJ, Cartmill JA, Cox MR, Adams SG, Martin CJ (2000) Grasper trauma during laparoscopic cholecystectomy. Aust N Z J Surg 70(8):578–581
9. Mirheydar HS, Parsons JK (2013) Diffusion of robotics into clinical practice in the united states: process, patient safety, learning curves, and the public health. World J Urol 31(3):455–461
10. Okamura AM (2004) Methods for haptic feedback in teleoperated robot-assisted surgery. Ind Robot Int J 31(6):499–508
11. Peters JH, Gibbons G, Innes J, Nichols K, Roby S, Ellison E (1991) Complications of laparoscopic cholecystectomy. Surgery 110(4):769–77
12. Sakellariou P, Protopapas AG, Voulgaris Z, Kyritsis N, Rodolakis A, Vlachos G, Diakomanolis E, Michalas S (2002) Management of ureteric injuries during gynecological operations: 10 years experience. Eur J Obstet Gynecol Reprod Biol 101(2):179–184
13. Sie A, Winek M, Kowalewski TM (2014) Online identification of abdominal tissues in vivo for tissue-aware and injury-avoiding surgical robots. In: 2014 IEEE/RSJ international conference on intelligent robots and systems (IROS 2014), IEEE, pp 2036–2042
14. Steele SR, Maykel JA, Champagne BJ, Orangio GR (2014) Complexities in colorectal surgery: decision-making and management. Springer, Berlin
15. Tholey G, Desai JP, Castellanos AE (2005) Force feedback plays a significant role in minimally invasive surgery: results and analysis. Ann Surg 241(1):102–109
16. Wagner CR, Stylopoulos N, Jackson PG, Howe RD (2007) The benefit of force feedback in surgery: examination of blunt dissection. Presence Teleoper Virtual Environ 16(3):252–262
17. Winkler A, Suchỳ J (2015) Implicit force control of a position controlled robot—a comparison with explicit algorithms. World Acad Sci Eng Technol Int J Comput Electr Autom Control Inf Eng 9(6):1454–1460
18. Yu X, Chizeck HJ, Hannaford B (2007) Comparison of transient performance in the control of soft tissue grasping. In: IEEE/RSJ international conference on intelligent robots and systems, 2007. IROS 2007, IEEE, pp 1809–1814